The Termination of the 1997–98 El Niño. Part I: Mechanisms of Oceanic Change*

GABRIEL A. VECCHI

NOAA/Geophysical Fluid Dynamics Laboratory, Princeton, New Jersey, and UCAR Visiting Scientist Program, Boulder, Colorado

D. E. HARRISON

Joint Institute for the Study of the Atmosphere and Oceans, University of Washington, and NOAA/Pacific Marine Environmental Laboratory, Seattle, Washington

(Manuscript received 11 February 2005, in final form 14 September 2005)

ABSTRACT

The 1997–98 El Niño was both unusually strong and terminated unusually. Warm eastern equatorial Pacific (EEqP) sea surface temperature anomalies (SSTAs) exceeded 4°C at the event peak and lasted well into boreal spring of 1998, even though subsurface temperatures began cooling in December 1997. The oceanic processes that controlled this unusual termination are explored here and can be characterized by three features: (i) eastward propagating equatorial Pacific thermocline (Z_{tc}) shoaling beginning in the central Pacific in November 1997; (ii) persistent warm EEqP SSTA between December 1997 and May 1998, despite strong EEqP Z_{tc} shoaling (and subsurface cooling); and (iii) an abrupt cooling of EEqP SSTA in early May 1998 that exceeded 4°C within two weeks.

It is shown here that these changes can be understood in terms of the oceanic response to changes to the meridional structure of the near-equatorial zonal wind field. Equatorial near-date-line westerly wind anomalies greatly decreased in late 1997, associated with a southward shift of convective and wind anomalies. In the EEqP, equatorial easterlies disappeared (reappeared) in late January (early May) 1998, driving the springtime extension (abrupt termination) of this El Niño event. The authors suggest that the wind changes arise from fundamentally meridional processes and are tied to the annual cycle of insolation.

1. Introduction

The primary modes of tropical Pacific coupled ocean–atmosphere system variability on seasonal to interannual time scales are related to the El Niño–Southern Oscillation (ENSO) phenomenon (e.g., Weare et al. 1976; Rasmusson and Carpenter 1982; Cane 1983; Harrison and Larkin 1996, 1998a; Larkin and Harrison 2002). The ENSO phenomenon is of intrinsic scientific interest and is also of social relevance because of its associated large-scale changes in regional biological productivity (e.g., Barber and Chavez 1986; Chavez et al. 1998; Strutton and Chavez 2000; Wilson and Adamec 2001; Radenac et al. 2001) and global weather patterns (Bjerknes 1966, 1969; Donguy and Henin 1980; Rasmusson and Wallace 1983; Nicholls and Kariko 1993; Harrison and Larkin 1998b). The air–sea interactions that bring about El Niño equatorial Pacific sea surface temperature anomaly (SSTA) changes have been studied intensively for many years and remain the focus of much interest at present [see the special issue of *Journal of Geophysical Research*, 1998, Vol. 103, No. C7, and Wang and Picaut (2004) for reviews of recent El Niño research]. Understanding these coupled mechanisms is essential to improving our understanding and prediction of El Niño. Here we focus on the oceanic mechanisms that led to the cooling of eastern equatorial Pacific (EEqP) SSTA at the end of the recent 1997–98 El Niño event.

The termination of the 1997–98 El Niño event was interesting in many ways [see McPhaden (1999), Wang and Weisberg (2000), and Picaut et al. (2002) for detailed observational descriptions of the entire 1997–98

* Joint Institute for the Study of the Atmosphere and Ocean Contribution Number 943 and Pacific Marine Environmental Laboratory Contribution Number 2518.

Corresponding author address: Dr. Gabriel A. Vecchi, NOAA/Geophysical Fluid Dynamics Laboratory, Princeton University, Forrestal Campus, Rte. 1, P.O. Box 308, Princeton, NJ 08542-0308. E-mail: Gabriel.A.Vecchi@noaa.gov

El Niño] and was problematic for many of ENSO forecast systems (e.g., Barnston et al. 1999; Landsea and Knaff 2000). The EqP thermocline depth (Z_{tc}) began shoaling in December 1997 in the central Pacific and EEqP subsurface temperatures continued to cool through May 1998. In general, there is a fairly strong positive correlation between SSTA and Z_{tcA} in the EEqP (e.g., Harrison and Vecchi 2001; Zelle et al. 2004; Zhang and McPhaden 2006), with deep (shallow) Z_{tc} associated with warm (cool) SST. However this relationship broke down in early to mid-1998, when the EEqP SST remained significantly warmer than normal through April 1998 while overlying anomalously cool subsurface waters [see McPhaden (1999), Zhang and McPhaden (2006), or the TAO data display online at http://pmel.noaa.gov/tao]. Then, dramatically and unexpectedly, SSTs cooled by over 4°C over the first two weeks of May 1998 (see McPhaden 1999; Takayabu et al. 1999; Picaut et al. 2002). More commonly, El Niño events terminate with SSTAs diminishing as the thermocline shoals so that EEqP SST is near normal by early spring (e.g., Harrison and Larkin 1998a; Harrison and Vecchi 2001).

The evolution of the EEqP Z_{tc} is an important dynamical and diagnostic component of the evolution of El Niño. Changes in EEqP Z_{tc} can directly impact SST through changes in vertical advection and mixing of temperature and are symptomatic of changes in the near-surface zonal current field (and thus zonal advection of temperature). Prior to the end of El Niño events Z_{tc} goes from being deeper than normal, to being close to or shallower than normal (see Harrison and Vecchi 2001). This Z_{tc} shoaling preconditions the termination of El Niño by making cold water available to the surface and is also often accompanied by an enhanced westward advection of cool water.

There have been many mechanisms suggested for the timing of the shoaling of Z_{tc} at the end of El Niño (see Neelin et al. 1998; Guilyardi et al. 2003; Wang and Picaut 2004; and references therein). "Oscillator" mechanisms that have been proposed to explain the phase turnabout of El Niño include the "delayed oscillator" (Zebiak and Cane 1987; Suarez and Schopf 1988; Battisti and Hirst 1989) in which a delayed negative feedback comes from the coupled response to oceanic waves reflected from the western boundary that are driven by the central Pacific wind response to the increased SSTs; the "advective–reflective oscillator" (Picaut et al. 1996, 1997), which emphasizes the roles of reflection off both the eastern and western boundaries and the zonal advection of temperature; the "west Pacific oscillator" (Weisberg and Wang 1997) in which the negative feedback involves the atmospheric response in the west Pacific to cold SST anomalies [the impact of off-equatorial west Pacific SST anomalies is also emphasized by Wang et al. (1999)]; and the "recharge oscillator" (Jin 1997), which is formulated through the integrated impacts of the negative feedbacks to the central and east Pacific wind response to SST anomalies. There also have been efforts to unify the processes in the proposed oscillator mechanisms into a single framework (e.g., Wang 2001). In these proposed mechanisms the EEqP Z_{tc} shoaling at the end of El Niño is brought about by integrated effects over the El Niño event, often set in motion by the same processes that bring about the Z_{tc} deepening.

Harrison and Vecchi (1999, henceforth HV99) and Vecchi and Harrison (2003, henceforth VH03) have offered a mechanism for the timing of the Z_{tc} shoaling at the end of El Niño events, which involves interactions between the annual cycle of insolation and El Niño conditions. Harrison (1987), Harrison and Larkin (1998a), and HV99 note that in the winter of every El Niño since the end of WWII, the central equatorial Pacific westerly wind anomalies—which are important to the onset and maintenance of waveguide warming in the east (e.g., Wyrtki 1975; Giese and Harrison 1991; Vecchi and Harrison 2000; Lengaigne et al. 2004)—move south of the equator and are no longer able to strongly force the oceanic equatorial waveguide. HV99 and VH03 suggest that the southward shift of the near-date-line wind anomalies results from the annual cycle of insolation, an interpretation supported by recent atmospheric general circulation model (AGCM) experiments (Spencer 2004; Vecchi 2006), as well as coupled general circulation model (CGCM) experiments (e.g., Vecchi et al. 2004; Lengaigne et al. 2006).

The processes that controlled the Z_{tc} evolution during the termination of the 1997–98 El Niño have been explored in a number of papers (e.g., McPhaden 1999; McPhaden and Yu 1999; Boulanger and Menkes 1999, 2001; Delcroix et al. 2000; Wang and Weisberg 2000; Vialard et al. 2001; Picaut et al. 2002; Boulanger et al. 2003; Boulanger et al. 2004). These studies suggest that the Z_{tc} changes during the termination of the 1997–98 El Niño event involved both the reflection of oceanic equatorial waves off eastern and western boundaries and changes directly forced by atmospheric wind stress variability. Many of the studies show that the Z_{tc} changes driven by zonal stress are larger (60%–80%) than those resulting from energy reflected off the boundaries.

There also is little consensus concerning the processes responsible for the unusual and abrupt return of

cold SST to the EEqP in May 1998. McPhaden (1999) speculated that the disappearance and reappearance of EEqP easterlies in February 1998 and May 1998, respectively, led to the unusual extension of warm SSTA and rapid cooling in May 1998. Takayabu et al. (1999) suggested that the rapid termination of the event in May 1998 was due to the passage of a Madden–Julian oscillation (MJO: see Madden and Julian 1994) event, through the easterlies that precede the convectively active phases of the MJO. Picaut et al. (2002) suggested that the abrupt cooling was due to oceanic processes involving a superposition of various wave modes and hypothesized that this resulted in sudden ocean mixing due to an increase in near-surface vertical current shears. These three different interpretations were suggested based on observationally based analyses, and the examination within a dynamically consistent framework presented here helps evaluate their relevance to 1997–98.

Here we here argue that many aspects of the termination of the 1997–98 El Niño can be understood in terms of the oceanic response to central and eastern equatorial wind changes rather than internal oceanic processes. The timing of the Z_{tc} shoaling at the end of the 1997–98 El Niño event followed the HV99 scenario. The resulting period of shallow Z_{tc} and warm SSTs in early 1998 in the EEqP resulted from the disappearance of equatorial easterly trade winds in January 1998. The rapid cooling in May 1998 was driven by a rapid return of equatorial easterlies and their associated equatorial upwelling and vertical mixing. The focus of this paper is the response of the ocean to changes in the atmospheric wind field in which the wind evolution is taken as given. Since El Niño is a coupled ocean–atmosphere phenomenon, the mechanisms that control the evolution of the winds are clearly of interest, and those are addressed in a companion paper, Vecchi (2006).

In the next section we describe the datasets used and the OGCM and Control experiment. In section 3 we explore the processes that drove the EEqP thermocline shoaling in late 1997/early 1998 through a series of perturbation OGCM experiments. In section 4 we explore the mechanisms that resulted in the extension and abrupt termination of the warm SSTA in the EEqP. Section 5 offers a summary of the results and a discussion.

2. Data and methods

a. Data

As our wind dataset we used the European Centre for Medium-Range Weather Forecasts (ECMWF) 10-m operational 12-h wind analysis on their 2.5° × 2.5° global grid (ECMWF 1989). We constructed a monthly climatology from the 12-h ECMWF surface wind analysis of the period 1986–2003, using a time axis centered on the middle day of each month. Anomalies are computed by subtracting the monthly climatology linearly interpolated in time. As a proxy for atmospheric convection we use the global 2.5° × 2.5° daily gridded OLR dataset provided by the National Oceanic and Atmospheric Administration–Cooperative Institute for Research in Environmental Sciences (NOAA–CIRES) Climate Diagnostics Center (available online at http://www.cdc.noaa.gov). We compute a monthly climatology by averaging over the years 1980–2003. Daily anomalies are computed by subtracting the monthly climatology linearly interpolated between the centers of each month. As our SST dataset we use the National Centers for Environmental Prediction (NCEP) weekly 1° × 1° SST optimal interpolation (OI) version 2 (Reynolds and Smith 1994; Reynolds et al. 2002); anomalies are computed by subtracting a climatology computed from 1981–2003. Using the Comprehensive Ocean–Atmosphere Data Set (COADS: Woodruff et al. 1987) 1946–93 climatology does not affect our SST results.

We use two observational datasets to characterize the evolution of the depth of the thermocline, which—throughout this paper—we will define to be the depth of the maximum vertical temperature gradient. Tropical Pacific subsurface temperatures are available for the period 1986–present from the Tropical Atmosphere Ocean (TAO) array (McPhaden 1993; McPhaden et al. 1998), which we use to compute the depth of the thermocline (Z_{tc}). Because the TAO subsurface temperature data have gaps in space and time, care must be taken when computing derived quantities, like Z_{tc}. We first meridionally average (from 2°S to 2°N) the TAO temperature data at each longitude and thermister depth and then fill in depth by linear interpolation. The depth of the thermocline is computed as the location of the maximum vertical gradient of 2°S–2°N temperature, which is always at an operating thermister location. The TAO Z_{tc} data is then linearly filled in time to span gaps of less than 15 days and averaged from 2°S to 2°N.

We also use the NOAA/Geophysical Fluid Dynamics Laboratory (GFDL) monthly tropical Pacific data assimilation product (Rosati et al. 1997) as another subsurface dataset with which to verify our modeling studies. To compute the thermocline depth using the GFDL assimilation product, we first average the temperature data from 2°S to 2°N and then compute the location of the maximum vertical gradient in temperature, taken to be the depth of the equatorial thermocline (Z_{tc}).

b. OGCM description

We performed a sequence of ocean general circulation model (OGCM) experiments to examine the forced response resulting from the specific wind changes during 1997–98. We use the NOAA/GFDL primitive equation OGCM, Modular Ocean Model version 2 (MOM2), versions of which have been used in many studies of the tropical Pacific (e.g., Philander and Seigel 1985; Harrison et al. 1990; Giese and Harrison 1991; HV99; Harrison et al. 2000; VH03). The model resolution is a uniform 1° in the zonal direction and ⅓° in the meridional between 10°S and 10°N, stretching to 2.5° by 30°S and 3° by 50°N. The model has 29 levels in the vertical with 10 levels in the upper 100 m; time stepping and topography were set up as in Harrison et al. (2000) and Vecchi and Harrison (2003). Vertical mixing was parameterized using the Richardson-number-dependent scheme of Pacanowski and Philander (1981). The adjustable parameters ν_0, α, and n were set to 5×10^{-3} m^2 s^{-1}, 0.5, and 1, respectively; the background diffusivity κ_b and viscosity ν_b were set at 1×10^{-4} and 1×10^{-5} m^2 s^{-1}, respectively; and the minimum wind stirring at the bottom of the surface grid cell was set to 1×10^{-3} m^2 s^{-1}. Horizontal mixing was parameterized as eddy diffusion with eddy viscosity coefficient A_υ of 1×10^3 m^2 s^{-1} and heat diffusion coefficient A_h of 2×10^3 m^2 s^{-1}. To initialize the model hindcast, the OGCM was spun up for 10 years using the monthly mean climatological wind stress field of Harrison (1989). Surface heat flux was parameterized, as in Harrison (1991), using the annual mean air temperature from the COADS climatology (Woodruff et al. 1987) computing air temperature based on the model SST and the historical air temperature SST (AIRT-SST) as a function of SST; spatially and temporally invariant stratus clouds are parameterized based on the Klein and Hartmann (1993) observational analysis of global marine stratus clouds. Sea surface salinity was restored to the annual mean Levitus (1982) climatology using a 50-day restoring time scale.

The hindcast was run, after this 10-yr spinup with climatology, using the 1996–98 wind forcing computed from the ECMWF 12-hourly, 2.5° × 2.5° resolution operational 10-m wind analysis. Surface momentum fluxes are parameterized using the bulk formulas of Large and Pond (1981). Surface latent and sensible heat fluxes are parameterized using the bulk formulas of Large and Pond (1982), computing air temperature based on the model SST and the historical (AIRT-SST) as a function of SST; spatially and temporally invariant stratus clouds are parameterized based on the Klein and Hartmann (1991) observational analysis of global marine stratus clouds. Sea surface salinity was restored to the annual mean Levitus (1982) climatology using a 50-day restoring time scale. For the bulk formulas, wind velocities are adjusted to velocities relative the ocean surface velocity by subtracting the vector velocity of the upper-ocean model grid cell because surface currents can be a nontrivial fraction of wind speed (e.g., Kelly et al. 2001).

Figure 1 shows the evolution of the monthly smoothed observed and hindcast SST and Z_{tc} at three locations in the EEqP (140°, 125°, and 110°W). Generally, the timing and amplitude of the simulated changes are comparable to those observed. Throughout the EEqP the thermocline begins shoaling between November 1997 and December 1997, while SST remains warm through May 1998. The rapid surface cooling in all three locations is reproduced well by the OGCM. It is worth noting that, while the OGCM simulation suffers from a too diffuse thermocline (a common problem with most z-coordinate dynamical ocean models), the location of the maximum gradient of temperature closely follows observations. We have performed the experiments described here using slightly different model configurations, and none of the fundamental results is altered.

3. Equatorial Pacific thermocline shoaling processes

Figure 2 shows the evolution of the meridional structure of the near-date-line wind anomaly field from the 1997–98 El Niño; this figure is a reproduction of Fig. 1b from HV99. The characteristic southward wind anomaly shift evident in El Niño events is clear in the 1997–98 El Niño. As in other El Niño events (including the recent 2002–03 El Niño: VH03), the 1997–98 southward shift resulted in a significant reduction in the strength of the equatorial westerly anomalies (see Fig. 3a); though there are strong westerly anomalies at 5°S in January 1998, they are far enough from the equator to drive a limited equatorial Kelvin response. Even though the central equatorial Pacific zonal wind anomalies do not become negative (easterly) until March 1998, they are greatly reduced (from 6 m s^{-1} to close to zero) by November 1997. The weak westerly anomalies in the far western equatorial Pacific become slightly easterly beginning November 1997 (Fig. 3a, red line); yet the change in stress anomaly in the west Pacific is much less than that in the central Pacific.

Eastward propagating shoaling of the equatorial Pacific Z_{tc} began near the date line following the southward shift. Figure 3b shows the time–longitude evolution of the 2°S–2°N time rate of change of Z_{tc} from the

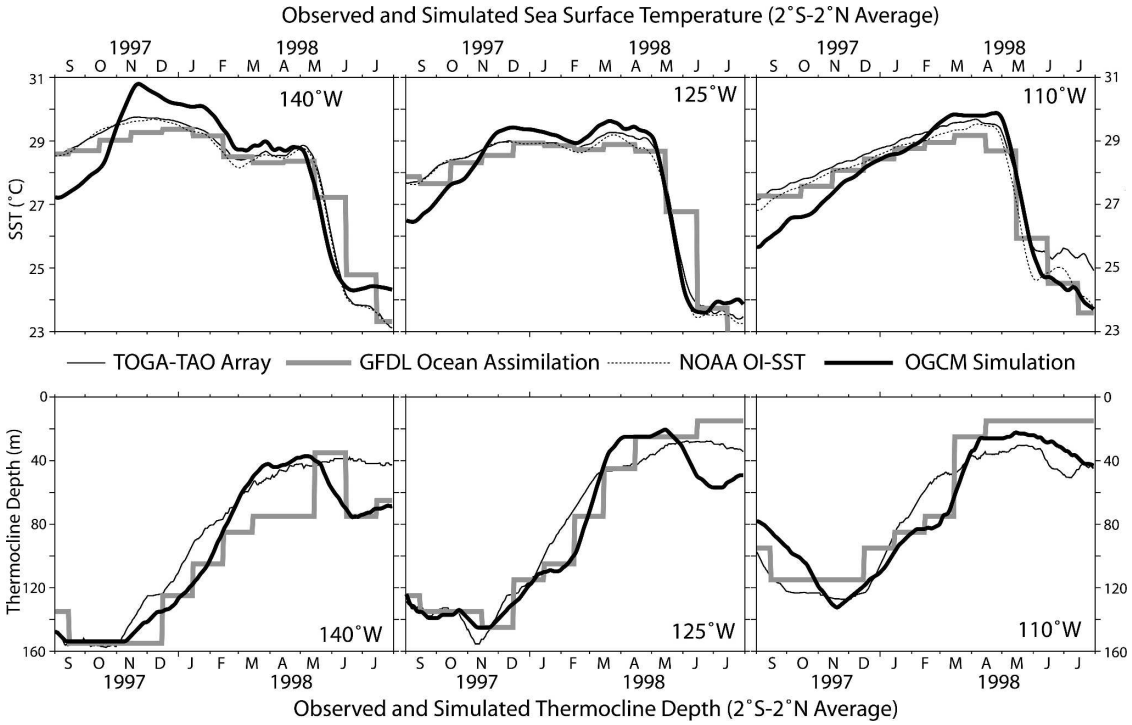

FIG. 1. Time series of observed and model hindcast eastern equatorial Pacific Ocean evolution during the height and termination of the 1997–98 El Niño event (at three locations: 140°, 125°, and 110°W; averaged between 2°S and 2°N). (a), (b), (c) 1-m temperatures from the TAO moored buoys (thin solid line), SST from the NOAA–NCEP OI SST product (dotted line), and temperature of the shallowest GFDL Ocean Assimilation grid box (0–10 m; gray line); temperature of the shallowest OGCM grid box (0–10 m; dark line); units are °C. (d), (e), (f) Depth of the thermocline from the TAO moored buoys (light line), the GFDL Ocean Data Assimilation product (gray line), and the OGCM (dark line): units are meters. Parameters from the GFDL Ocean Assimilation are monthly means, while parameters from the other datasets are smoothed with a 31-day boxcar smoother.

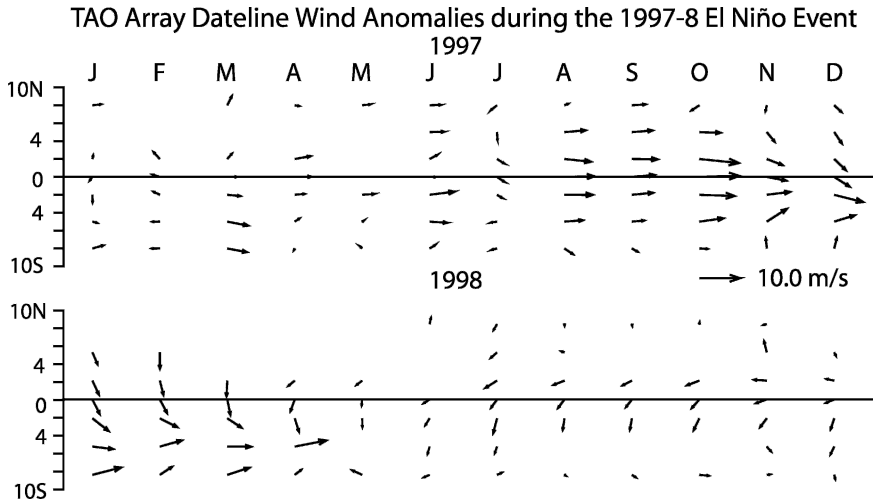

FIG. 2. Evolution of the monthly mean date line (180°) 4-m wind anomalies observed by the TAO moored buoys throughout the 1997–98 El Niño. Anomalies are computed relative the COADS monthly climatology. Scale vector is 10 m s^{-1}. Notice the southward shift of the zonal wind anomalies beginning November 1997.

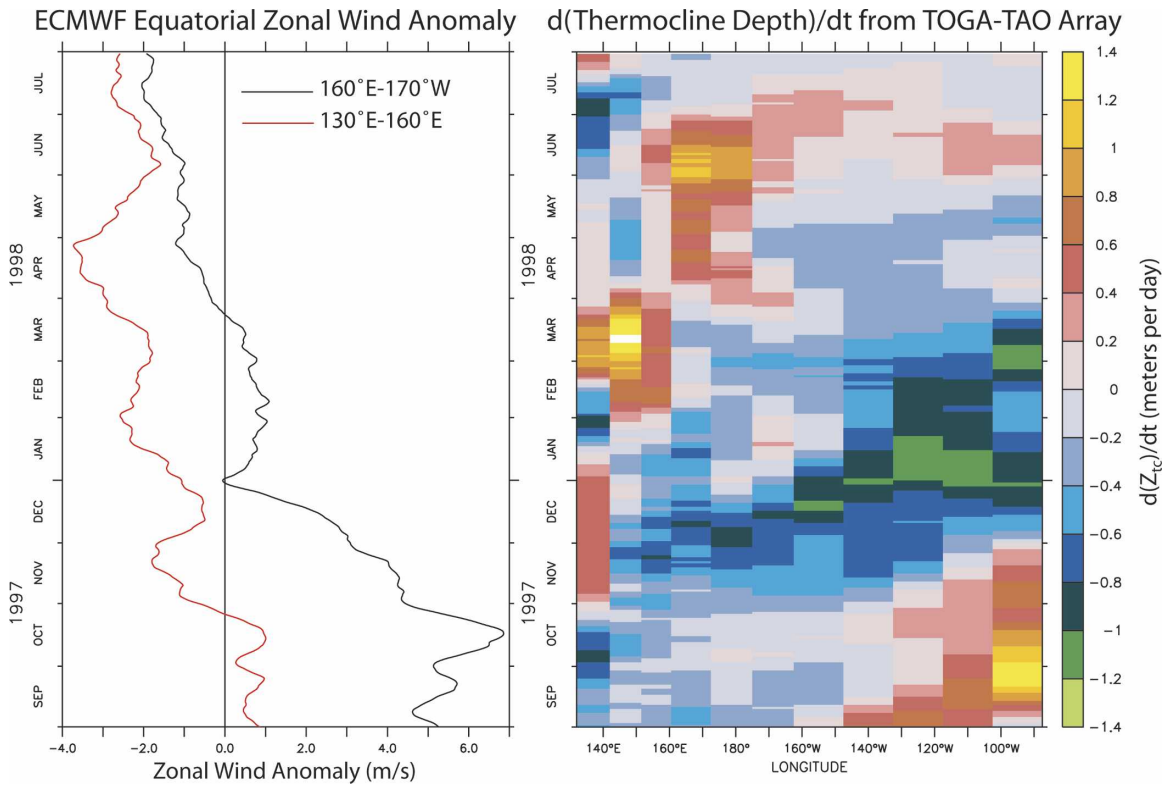

FIG. 3. (left) Time series of the 31-day running mean equatorial zonal wind anomaly in the near-date-line Pacific (black line) and in the far-west Pacific (red line). Units are m s^{-1}. Notice the strong reduction in near-date-line zonal wind anomaly beginning October 1997. (right) Time–longitude map evolution of the time rate of change of the depth of the thermocline (averaged between 2°S and 2°N) from the TAO mooring array throughout the 1997–98 El Niño. Units are m day^{-1}; warm colors indicate deepening and cool colors indicate shoaling; data smoothed by a 91-day boxcar in time. See text for discussion.

TAO array during 1997–98. The equatorial Z_{tc} signal seems to propagate eastward at a speed consistent with that expected in the linear oceanic response to equatorial wind changes (e.g., Anderson and Gill 1976; Cane 1977; Moore and Philander 1977), somewhere between 2.2 and 2.7 m s^{-1}. The Z_{tc} shoaling does not appear to have originated at the western boundary. The timing and structure of the observed Z_{tc} evolution at the end of the 1997–98 El Niño is consistent with that expected from the HV99 mechanism.

To explore the extent to which the thermocline shoaling can be explained as the forced response to this southward shift, we have performed a series of experiments in which the wind anomaly field is modified; Table 1 summarizes the wind anomaly forcing used in each of these perturbation experiments. The experiments involve holding some components of the wind anomaly field at the mean October 1997 values beginning October 1997 throughout the model integration and allowing other components of the wind anomaly field to follow the observed 12-hourly data; the anomalies are added to the climatological winds before forcing the model.

First, we performed three experiments (named FIXED, TY, and TX) to test the extent to which the Z_{tc} evolution could be understood as a response to basin-wide zonal wind anomaly changes, compared to that forced by changes in the meridional wind anomaly field

TABLE 1. Description of the wind anomaly fields used in the perturbation OGCM experiments described in section 3.

Expt	Zonal stress anomaly	Meridional stress anomaly
FIXED	Fixed	Fixed
TY	Fixed	Variable
TX	Variable	Fixed
WCPTX	West of 150°W between 5°S and 5°N: variable elsewhere: fixed	Fixed
INV-WCPTX	West of 150°W between 5°S and 5°N: fixed elsewhere: variable	Variable
CPTX	From 160°E to 150°W between 5°S and 5°N: variable elsewhere: fixed	Fixed
INV-CPTX	From 160°E to 150°W between 5°S and 5°N: fixed elsewhere: variable	Variable

and through the integrated forcing up to the wind shift in November 1997. In experiment FIXED both zonal and meridional wind anomalies are held at the mean October 1997 values beginning October 1997 to show the response of the ocean to the integrated forcing up to October 1997. In experiment TY the zonal wind anomalies are held at the mean October 1997 values beginning October 1997, while in experiment TX the meridional wind anomalies are held constant; these experiments show the impact of the wind anomaly changes beginning in October 1997 on the evolution of the system.

We expect from the mechanism of HV99 and the results of VH03, and from the observed evolution of the wind anomaly and Z_{tc} anomaly field (Figs. 2 and 3), that in experiments FIXED and TY the Z_{tc} shoaling will be greatly reduced, while in experiment TX the Z_{tc} shoaling should be similar to the full Control hindcast. Meanwhile, the principal alternative hypotheses (the various oscillator paradigms) involve coupled processes integrated over many months and imply that the timing of the shoaling should be little affected by the removal/presence of the southward shift.

Figure 4 shows the evolution of the model Z_{tc} at 110°W for the Control run and these three perturbation experiments (FIXED, TX, and TY). There is a significant shoaling of the EEqP Z_{tc} only in the model runs that include the zonal wind anomaly changes (the Control and experiment TX). Both the model hindcast (dark black line) and experiment TX (crossed line) exhibit Z_{tc} shoaling beginning in late 1997, continuing through April 1998. This Z_{tc} evolution is similar to that measured by the TAO array and of the GFDL data assimilation product (see Fig. 1). For perturbation experiments FIXED and TY there is negligible EEqP Z_{tc} shoaling through April 1998. Thus, in this model hindcast, the timing of the rapid EEqP Z_{tc} shoaling at the end of the 1997–98 El Niño event was not driven by integrated processes but was the direct response to a change in the zonal wind anomaly field following October 1997.

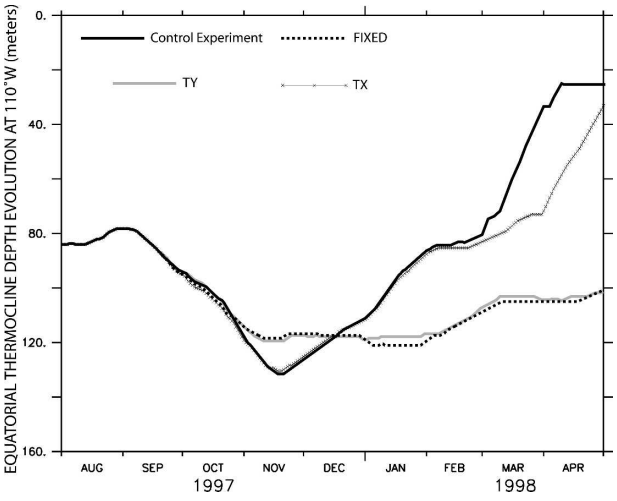

FIG. 4. Time series of the depth of the thermocline at 110°W (averaged 2°S–2°N and smoothed with a 31-day smoother) from the Control OGCM experiment (dark solid line), and perturbation experiments FIXED (dashed line), TY (gray line), and TX (crossed line). Notice that the timing of the Z_{tc} shoaling is set by the zonal wind anomaly forcing in late 1997. Units are meters.

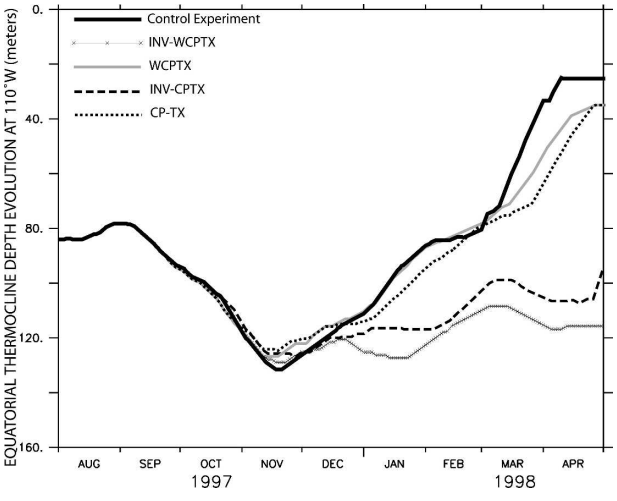

FIG. 5. Time series of the depth of the thermocline at 110°W (averaged 2°S–2°N and smoothed with a 31-day smoother) from the Control OGCM experiment (dark solid line), from the perturbation experiments WCPTX (crossed line), INV-WCPTX (gray line), CPTX (dashed line), and INV-CPTX (dotted line). Notice that the shoaling of the Z_{tc} is set by the late 1997 evolution of the zonal wind anomalies in the region 5°S–5°N, 160°E–150°W; the southward shift of central Pacific zonal wind anomalies off the equator drove the Z_{tc} shoaling at the end of 1997. Units are meters.

To isolate the extent to which the change in zonal wind anomalies in the near-date-line Pacific were those that set the timing to the Z_{tc} shoaling we performed four additional experiments. These additional experiments involve holding the mean October 1997 wind anomalies over partial regions of the Pacific basin; the wind anomaly forcing field for each of these experiments is listed in Table 1. In the first pair of experiments, named WCPTX and INV-WCPTX, we explore the impact of the zonal wind anomalies west of 150°W, between 5°S and 5°N. In the second experiment pair, named CPTX and INV-CPTX, we isolate the impact of the zonal wind anomalies between 160°E and 150°W.

Figure 5 shows the evolution of the Z_{tc} at 110°W between 2°S and 2°N from the Control and four additional perturbation experiments (WCPTX, INV-

WCPTX, CPTX, and INV-CPTX). In experiments INV-WCPTX and INV-CPTX—where the near-date-line zonal wind anomaly changes are absent—there is little thermocline shoaling in the EEqP. Meanwhile, in both experiments WCPTX and CPTX—where the near-date-line zonal wind anomaly changes are present—the thermocline shoaling is comparable to that in the full hindcast. The impact of the weak far-west Pacific zonal wind anomaly changes (seen in Fig. 2) can be seen in the difference between experiments WCPTX and CPTX and between INV-WCPTX and INV-CPTX. It is evident that the far-west Pacific zonal wind anomaly changes contributed to the thermocline shoaling, but their impact was much smaller than that of the near-date-line zonal wind anomaly changes. Thus, the principal control of the timing of the Z_{tc} shoaling at the end of the 1997–98 El Niño event was the strong weakening of zonal wind anomalies of the near-date-line zonal wind anomaly field beginning November 1997.

4. Eastern equatorial Pacific SST change processes

Here we explore the mechanisms that led to this unusual shallow Z_{tc}/warm SSTA period and the return of normal SST to the EEqP. The cooling of the SST in the boreal spring of 1998 was most dramatic between 140° and 110°W. Figure 6 summarizes the evolution of the ocean–atmosphere system at 110°W between 2°S and 2°N: that location is representative of the evolution across the eastern equatorial Pacific, and it has relatively homogeneous TAO subsurface data coverage over the period. Presented are the ECMWF 10-m zonal winds (U_{10m}) along with the climatological winds (based on 1986–2003), the NCEP weekly SST along with its monthly climatology (based on 1982–2003), and the Z_{tc} from the TAO array averaged between 2°S and 2°N.

Based on these three quantities (U_{10m}, SST, and Z_{tc}), the termination of the 1997–98 El Niño can be decomposed into three periods. The first period—before January 1998—was characterized by a deep (anomalies >80 m) Z_{tc} (which began to shoal in December 1997), and warm SSTs; this represents the prototypical developed El Niño situation, evident in many schematic descriptions of El Niño. The second period—between January and May 1998—had shallow Z_{tc}, no easterlies, and warm SSTs; this period was highly unusual based on the historical record. The final period—following May 1998—had shallow Z_{tc}, easterlies, and cold SSTs; this represents the return to the dominant mean relationships between these three parameters. Throughout the entire period there was moderate local subseasonal

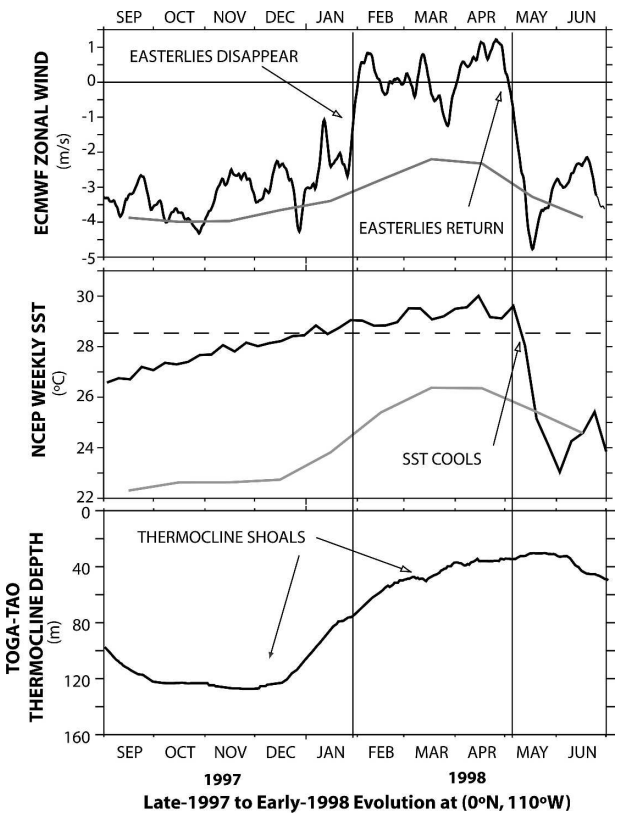

FIG. 6. Time series of the observed ocean–atmosphere evolution at 110°W (averaged 2°S–2°N) at the end of the 1997–98 El Niño. (a) Fifteen-day smoothed zonal wind from the ECMWF operational analysis (solid) and monthly climatology (dashed); units are m s^{-1}. (b) Weekly SST from the NOAA–NCEP OI product (solid) and monthly climatology; units are °C. (c) Thirty-one-day smoothed thermocline depth from the TAO moored buoy; units are meters.

zonal wind variability at 110°W with peak-to-trough amplitudes of close to 2 m s^{-1}; this is the average amplitude of intraseasonal wind variability associated with the MJO in the EEqP (e.g., Hendon and Salby 1994).

We suggest that changes in the local zonal wind field acted to extend the event into May of 1998 and then abruptly terminate it. First, as the Z_{tc} shoaled through January 1998, making cold water available to the shallow upwelling circulation, the easterlies disappeared, effectively decoupling the surface and subsurface of the eastern equatorial Pacific because there was no wind-forced upwelling. When the easterlies returned in May 1998, the surface and subsurface of the eastern equatorial Pacific were coupled again because the thermocline was shallow and the surface rapidly cooled through enhanced vertical mixing and upwelling, ending the El Niño event.

We ran a perturbation OGCM experiment, called HOLD-EAST, to test the hypothesis that the disap-

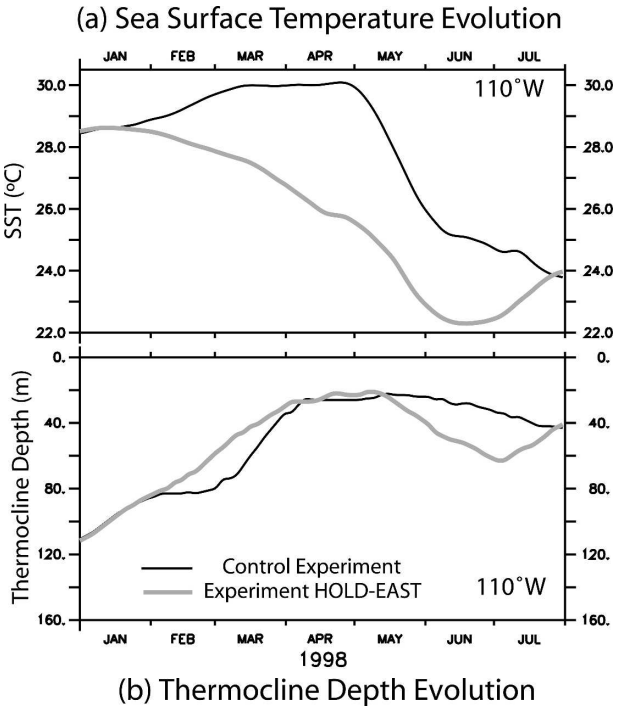

FIG. 7. Time series of the evolution of the OGCM at 110°W (averaged 2°S–2°N and smoothed with a 31-day boxcar) from the Control experiment (dark line) and the perturbation experiment in which the zonal winds east of 150°W are held at their 15 Dec 1997–15 Jan 1998 average value (i.e., in which the EEqP easterlies do not disappear; light line). (a) Evolution of the temperature at the uppermost ocean grid box (0–10 m); units are °C. (b) Depth of the thermocline; units are meters. Notice that the disappearance of easterlies—which happened in mid-January 1998—allowed the subsurface to cool without cooling the surface, as would have happened had the easterlies remained.

pearance of equatorial easterlies in the eastern equatorial Pacific (from late January 1998 until early May 1998) extended the El Niño event. In this experiment, the EEqP zonal winds (those east of 150°W) beginning January 1998 are held at the 15 December 1997 through 15 January 1998 average. Meanwhile, the meridional winds throughout the basin and the zonal winds west of 150°W are allowed to evolve as in the Control experiment.

Figure 7 shows the evolution of the (2°S–2°N, 110°W) SST and Z_{tc} for the Control experiment and for experiment HOLD-EAST. In both experiments Z_{tc} shoals throughout the entire period, with comparable amplitudes and timings. This is to be expected, as it was shown in the previous section that the Z_{tc} shoaling was principally controlled by central and west Pacific zonal wind anomaly changes, which were the same in the Control and HOLD-EAST experiments.

The evolution of SST in the two experiments, however, is remarkably different. In the Control experiment SST remains warm as the Z_{tc} shoals in early 1998, but, in experiment HOLD-EAST, SST cools as the Z_{tc} shoals. The EEqP upwelling and vertical mixing in the Control experiment are practically eliminated by the disappearance of the easterlies, while in experiment HOLD-EAST there is both significant EEqP upwelling and vertical mixing of temperature, which leads to the surface cooling seen in Fig. 7. Thus, the disappearance of EEqP easterlies in early 1998 decoupled the surface and subsurface waters, leading to a period of shallow Z_{tc} and warm SSTs in early 1998.

To test the hypothesis that the return of easterlies to the eastern equatorial Pacific in early May 1998 rapidly cooled the ocean, a series of perturbation experiments are run where the May 1998 winds are made to arrive earlier or later. To make the May 1998 winds arrive earlier, the wind record is truncated after a given month before April, for example, February 1998, and the May 1998 and subsequent winds are appended to the end of the record. So the sequencing of the twice-daily wind field would look as follows in this illustrative case:

$$\ldots \text{Jan98} \rightarrow \text{Feb98} \rightarrow \text{May98} \rightarrow \text{Jun98} \ldots .$$

To delay the arrival of the May winds, the April 1998 winds are repeated the number of months we wish to delay the arrival of May 1998. For example, to delay the arrival of May by two months, April is repeated twice:

$$\ldots \text{Mar98} \rightarrow \text{Apr98} \rightarrow \text{Apr98} \rightarrow \text{Apr98} \rightarrow \text{May98} \rightarrow \text{Jun98} \ldots .$$

We label these experiments MAY(−4) through MAY(−1), and MAY(1) through MAY(4). For experiments MAY(−4) through MAY(−1) the May 1998 winds are advanced 4, 3, 2, and 1 months, and for experiments MAY(1) through MAY(4) the May 1998 winds are delayed 1, 2, 3, and 4 months.

The hypothesized mechanism implies that advancing or delaying the arrival of the May 1998 winds will advance or delay the cooling of east Pacific SST in a coherent fashion. Figure 8 shows the evolution of SST and mean temperature in the upper 100 m at 110°W (2°S–2°N) for the perturbation experiments MAY(−4) through MAY(4) (light lines) and for the Control run (dark black line). In the Control run there is a sharp cooling of the surface and associated decrease in 0–100-m heat content, as the easterlies abruptly return in early May 1998. In each of the perturbation experiments the abrupt surface cooling, and 0–100-m heat content reduction, is evident as well, with the timing of the cooling set by the return of the easterlies. Thus, the cooling of eastern equatorial Pacific SSTs happened when, and only when, the easterlies returned.

The near-surface cooling was driven principally by

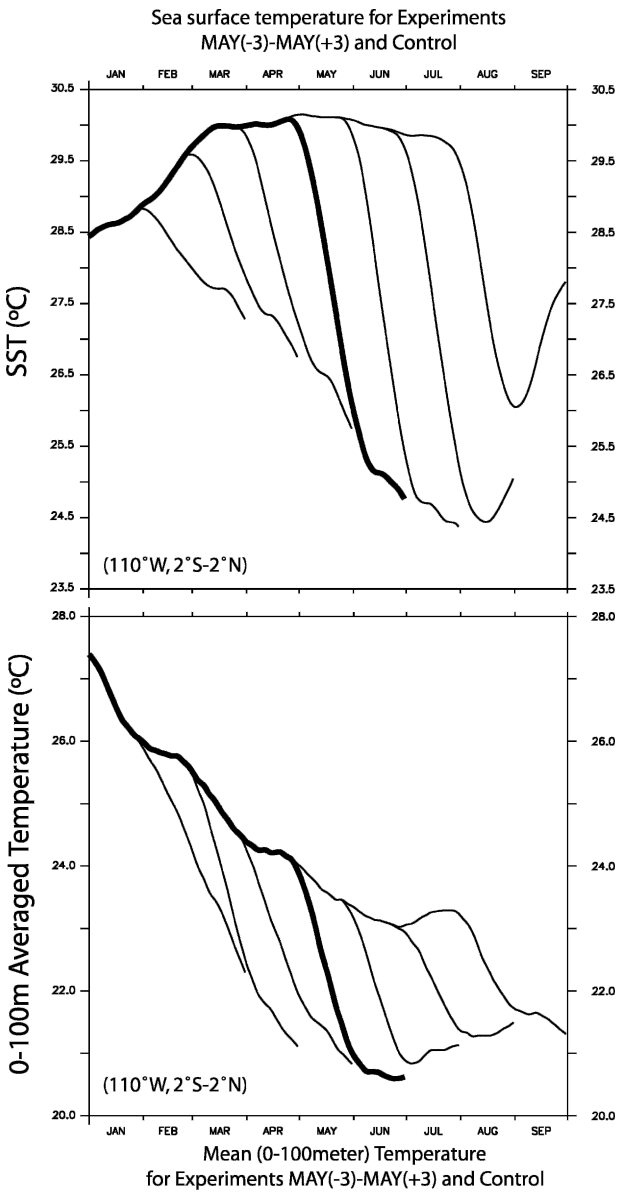

FIG. 8. Time series of the evolution of the OGCM at 110°W (averaged 2°S–2°N and smoothed with a 31-day boxcar smoother) from the Control experiment (dark line), and the suite of perturbation experiments in which the May 1998 winds are advanced or delayed by different number of months (lighter lines). (a) Evolution of the temperature at the uppermost ocean grid box (0–10 m); units are °C. (b) Depth of the thermocline; units are meters.

vertical advection, with vertical mixing of temperature as the second leading term, as the easterlies returned and recoupled the surface to the subsurface. The disappearance of the easterlies acted to decouple the surface and surbsurface by reducing vertical mixing and eliminating equatorial upwelling. It is clear from these experiments that the SST cooling in May 1998 was the response of the ocean to wind forcing and not due to internal oceanic mechanisms. However, the amplitude of the cooling in each of the perturbation experiments is roughly inversely proportional to the heat content of the upper 100 m. Thus, the ocean structure (with a very shallow Z_{tc}/low upper-ocean heat content in May 1998) preconditioned the system for the dramatic SST cooling observed in May 1998. The *timing* of the cooling in May 1998, however, was driven by the return of the easterlies.

5. Summary and discussion

Observational evidence and a series of focused OGCM experiments indicate that the characteristics of the termination of the 1997–98 El Niño can be explained in terms of the oceanic response to wind changes in the near-equatorial Pacific. A southward shift in November 1997 of the near-date-line westerly wind anomalies drove an eastward propagating shoaling of the equatorial thermocline that lasted well into the boreal spring of 1998. However, SST in the eastern equatorial Pacific (EEqP) did not cool in early 1998 because the local easterlies had disappeared, eliminating equatorial upwelling and so decoupling the warm surface ocean from the cooling subsurface. This decoupling allowed the combination of warm SST and cool subsurface temperatures to persist into May 1998. The return of easterlies in May of 1998 recoupled the surface to the subsurface and returned EEqP SST to normal values, ending the El Niño event.

The initial part of this termination is now familiar. A southward shift of equatorial westerly anomalies near the date line in boreal winter is characteristic of El Niño events (e.g., Harrison 1987, Harrison and Larkin 1998a; HV99; Larkin and Harrison 2002; VH03). The forced thermocline shoaling in the cold tongue over the following months has been discussed as a general aspect of El Niño termination by HV99, and shown to apply to the 2002–03 event by VH03. Although there is equatorial atmospheric variability on many time and space scales during El Niño events, the characteristic southward shift is capable of forcing the multimonth cold tongue thermocline shoaling with the timing and amplitude that are observed (see section 3).

Other recent work has also argued that the observed EEqP Z_{tc} shoaling at the end of the 1997–98 El Niño principally resulted from oceanic response to wind changes, rather than to wave reflection (McPhaden and Yu 1999; Boulanger and Menkes 1999, 2001; Delcroix et al. 2000; Wang and Weisberg 2000; Vialard et al. 2001; Picaut et al. 2002; Boulanger et al. 2003, 2004). Many of these studies noted that there was a reversal of the zonal wind anomaly field in the far-western equa-

torial Pacific (west of 150°E)—from being weakly (0–2 $m\,s^{-1}$) westerly to weakly (0–2 $m\,s^{-1}$) easterly—and attribute the shoaling to that change. It can be seen in Fig. 3 that the changes in the zonal wind anomalies near the date line, arising from the southward wind anomaly shift, are of much larger amplitude than those in the west Pacific.

Though the reduction of the central equatorial Pacific westerly anomalies can go far in explaining the timing of the thermocline shoaling in the EEqP, the full details of the evolution involve many aspects of the coupled system. As was seen in HV99, the southward shift of near-date-line zonal wind anomalies can explain the return to climatological thermocline depths in the EEqP, but the overshoot beyond climatology requires other processes; in the HV99 experiments one such process was the reflection of Rossby waves off the western boundary of the Pacific. In addition, changes in the far-west Pacific zonal wind anomaly field did play a role in the termination of the 1997–98 El Niño, even though the OGCM experiments described in section 3 indicate that the near-date-line zonal wind anomaly changes were dominant in setting the timing of the EEqP Z_{tc} shoaling. West Pacific wind changes may play a role, in general, in the termination of El Niño events (e.g., Guilyardi et al. 2003). Furthermore, it has also been argued by McPhaden and Yu (1999) that wind-generated upwelling Rossby waves are important in the evolution of the EEqP. The detailed character of the evolution of EEqP Z_{tc} in an El Niño event involves many processes.

Changes in the EEqP zonal wind field resulted in the delayed and dramatic termination of the 1997–98 El Niño. The sequence of experiments described in section 4 reveals that the disappearance of surface easterlies in early 1998 decoupled the warm surface ocean from the cooling subsurface, and led to the continuation of warm-pool level warm SSTA into spring (experiment HOLD-EAST). Other experiments [MAY(−4) through MAY(4)] establish that it was the upwelling and vertical mixing driven by the return of easterlies in May 1998 that recoupled the surface and subsurface and returned cold tongue SST to normal values. Our model studies establish a dynamical basis for the inferred cooling mechanism of Wang and McPhaden (2001) as well as demonstrating, within a dynamically consistent and physically complete framework, the critical importance of equatorial zonal wind changes, as hypothesized by McPhaden (1999), in the termination of 1997–98. Recently, Zhang and McPhaden (2006) use different methodology to also conclude that the disappearance and return of EEqP easterlies played the fundamental role described here.

In this study we have taken the variability of near-equatorial wind as given. The tropical Pacific is, however, a coupled atmosphere–ocean system, and we now briefly take on the topic of the mechanisms that were responsible for the evolution of the near-equatorial Pacific winds in 1997–98. The mechanisms behind the wind changes described here are addressed in a companion paper (Vecchi 2006).

The reduction of central Pacific equatorial zonal wind anomalies resulted from the southward shift of the zonal wind anomalies from being centered about the equator to being centered south of the equator. That the annual cycle of solar heating could account for the near-date-line southward shift of westerly anomalies has been argued previously based on observations (HV99; VH03), atmospheric model studies (Spencer 2004), and coupled model experiments (Vecchi et al. 2004; Lengaigne et al. 2006).

What accounted for the absence of EEqP easterly winds between January and May 1998 and the timing of the return of equatorial easterlies in May 1998? The disappearance of EEqP easterlies is not typical of most El Niño events, which tend to have their strongest zonal wind anomalies in the western and central Pacific and only weak zonal wind anomalies in the EEqP (e.g., Wyrtki 1975, Rasmusson and Carpenter 1982; Harrison and Larkin 1998a; Larkin and Harrison 2002). Takayabu et al. (1999) suggest (based on analysis of satellite wind, rainfall, and SST data) that the return of the easterlies in May 1998 resulted from the propagation of easterly winds on the leading edge of the convectively active part of a MJO (see Madden and Julian 1994) into the EEqP.

We propose an alternative hypothesis in which the annual cycle of insolation and the extreme SST anomalies of 1997–98 play a fundamental role. Figure 9 shows the time–latitude evolution EEqP zonal wind and outgoing longwave radiation (a proxy for atmospheric convection) through the termination of the 1997/98 El Niño. Prior to the disappearance (reappearance) of equatorial easterlies in late January (early May) 1998, there was a meridional migration of the zones of maximum convection onto (north of) the equator; the maximum westerly winds (weakest easterlies) can be seen to follow the location of the ITCZ onto and off the equator. We suggest that the disappearance (reappearance) of equatorial easterlies in January (May) 1998 was driven by the development (northward retreat) of an equatorial ITCZ, associated with the annual cycle of insolation. This suggestion is further explored in Vecchi (2006).

In summary, changes in the meridional structure of the zonal wind field were fundamental to the termina-

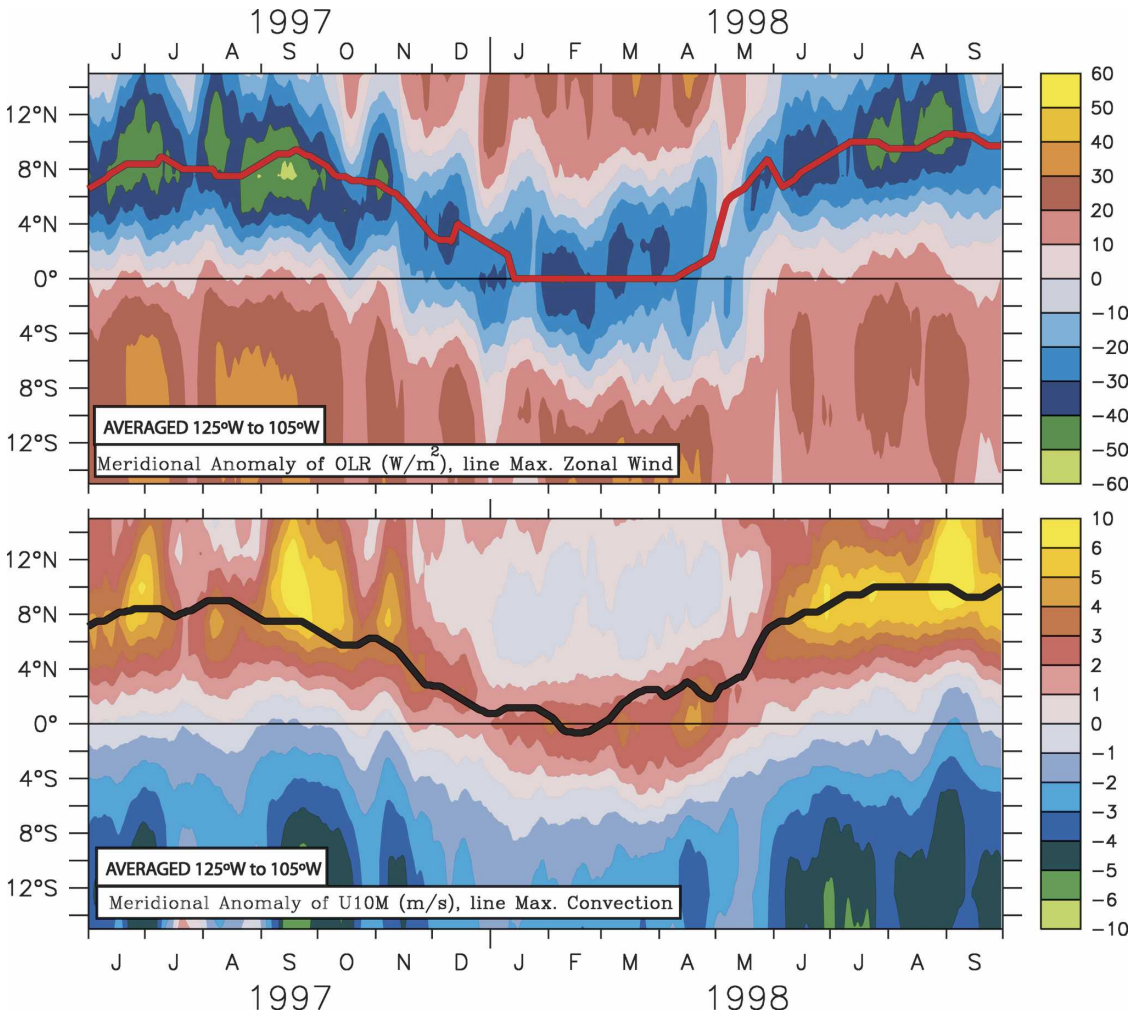

FIG. 9. Time–latitude evolution of the meridional anomaly (local value minus the meridional mean at each time point; averaged 120°–100°W and 90-day boxcar smoothed) of (a) the NOAA interpolated OLR product (units are W m^{-2}; low values indicate enhanced convection) and (b) zonal winds from the ECWMF operational analysis (units are m s^{-1}; high values indicate weak easterlies). Superimposed are the time series of (a) the meridional location of the max in zonal wind velocity (least easterly winds) and (b) the meridional location of the min in OLR (max in atmospheric convection). Notice the movement of the ITCZ onto the equator in January 1998, and off in May 1998.

tion of the 1997–98 El Niño event. A southward shift of near-date-line zonal wind anomalies in November 1997 drove eastward propagating thermocline shoaling, which preconditioned the cooling of EEqP SST. A disappearance (reappearance) of EEqP easterly winds drove the extension (rapid termination) of the warm EEqP SSTA into May 1998 and was associated with meridional changes in convection and wind. The character and timing of the atmospheric changes suggest that interactions between the annual cycle of insolation and anomalous El Niño conditions are a fundamental mechanism for the termination of El Niño events; improvements in our diagnosis and prediction of El Niño termination could come from explicit resolution of the seasonal variability in our dynamical El Niño models.

Acknowledgments. This research was supported by the Visiting Scientist Program at the National Oceanic and Atmospheric Administration's Geophysical Fluid Dynamics Laboratory (NOAA/GFDL) administered by the University Corporation for Atmospheric Research (UCAR), by the Joint Institute for the Study of the Atmosphere and Ocean (JISAO), under NOAA Cooperative Agreement NA17RJ11232, and by NOAA (OAR HQ and OGP). Analysis and graphics were done using freeware package Ferret (http://ferret.wrc.noaa.gov/). We gratefully acknowledge the TAO project office for making the TAO data easily and readily available. The OLR and SST data made easily accessible by NOAA–CDC, Boulder, Colorado, are appreciated. Helpful comments, discussion, and suggestions

were given by N. Bond, M. Harrison, S. Ilcane, N.-C. "G" Lau, M. McPhaden, A. Rosati, and A. Wittenberg. We are grateful for the insightful comments and suggestions from E. Tziperman and two anonymous reviewers.

REFERENCES

Anderson, D. L. T., and A. E. Gill, 1976: Spin-up of a stratified ocean with applications to upwelling. *Deep-Sea Res.,* **22,** 583–596.

Barber, R. T., and F. P. Chavez, 1986: Ocean variability in relation to living resources during the 1982/83 El Niño. *Nature,* **319,** 279–285.

Barnston, A. G., M. H. Glantz, and Y. He, 1999: Predictive skill of statistical and dynamical climate models in SST forecast during the 1997–98 El Niño episode and the 1998 La Niña onset. *Bull. Amer. Meteor. Soc.,* **80,** 217–243.

Battisti, D. S., and A. C. Hirst, 1989: Internal variability in a tropical atmosphere–ocean model: Influence of basic state, ocean geometry and nonlinearity. *J. Atmos. Sci.,* **46,** 1687–1712.

Bjerknes, J., 1966: A possible response of the atmospheric Hadley circulation to equatorial anomalies in ocean temperature. *Tellus,* **18,** 820–829.

——, 1969: Atmospheric teleconnections from the equatorial Pacific. *Mon. Wea. Rev.,* **97,** 163–172.

Boulanger, J.-P., and C. Menkes, 1999: Long equatorial wave reflection in the Pacific Ocean from TOPEX/POSEIDON data during the 1992–1998 period. *Climate Dyn.,* **15,** 205–225.

——, and ——, 2001: The Trident Pacific model. Part 2: Role of long equatorial wave reflection on sea surface temperature anomalies during 1993–1998 TOPEX/POSEIDON period. *Climate Dyn.,* **17,** 175–186.

——, S. Cravatte, and C. Menkes, 2003: Reflected and locally wind-forced interannual equatorial Kelvin waves in the western Pacific Ocean. *J. Geophys. Res.,* **108,** 3311, doi:10.1029/2002JC001760.

——, C. Menkes, and M. Lengaigne, 2004: Role of high- and low-frequency winds and wave reflection in the onset, growth and termination of the 1997–1998 El Niño. *Climate Dyn.,* **22,** 267–280.

Cane, M. A., 1977: Forced baroclinic motions 1. Linear equatorial unbounded case. *J. Mar. Res.,* **34,** 629–665.

——, 1983: Oceanographic events during El Niño. *Science,* **222,** 1189–1194.

Chavez, F. P., P. G. Strutton, and M. J. McPhaden, 1998: Biological-physical coupling in the central equatorial Pacific during the onset of the 1997–98 El Niño. *Geophys. Res. Lett.,* **25,** 3543–3546.

Delcroix, T., B. Dewitte, Y. duPenhoat, F. Masia, and J. Picaut, 2000: Equatorial waves and warm pool displacements during the 1992–1998 El Niño Southern Oscillation events: Observation and modeling. *J. Geophys. Res.,* **105** (C11), 26 045–26 062.

Donguy, J. R., and C. Henin, 1980: Climatic teleconnections in the western South Pacific with El Niño phenomenon. *J. Phys. Oceanogr.,* **10,** 1952–1958.

ECMWF, 1989: The description of the ECMWF/WCRP level III-A global atmospheric data archive. Technical Attachment, 72 pp. [Available from ECMWF, Shinfield Park, Reading RG2 9AX, United Kingdom.]

Giese, B. S., and D. E. Harrison, 1991: Eastern equatorial Pacific response to three composite westerly wind types. *J. Geophys. Res.,* **96** (Suppl.), 3239–3248.

Guilyardi, E., P. Delecluse, S. Gualdi, and A. Navarra, 2003: Mechanisms for ENSO phase change in a coupled GCM. *J. Climate,* **16,** 1141–1158.

Harrison, D. E., 1987: Monthly mean island surface winds in the central tropical Pacific and El Niño. *Mon. Wea. Rev.,* **115,** 3133–3145.

——, 1989: On climatological monthly mean wind stress and wind stress curl fields over the world ocean. *J. Climate,* **2,** 57–70.

——, 1991: Equatorial sea surface temperature sensitivity to net surface heat flux: Some ocean circulation model results. *J. Climate,* **4,** 539–549.

——, and N. K. Larkin, 1996: The COADS sea level pressure signal: A near-global El Niño composite and time series view, 1946–1993. *J. Climate,* **9,** 3025–3055.

——, and ——, 1998a: The ENSO surface temperature and wind signal: A near-global composite and time-series view, 1946–1995. *Rev. Geophys.,* **36,** 353–399.

——, and ——, 1998b: Seasonal U.S. temperature and precipitation anomalies associated with El Niño: Historical results and comparisons with 1997–98. *Geophys. Res. Lett.,* **25,** 3959–3962.

——, and G. A. Vecchi, 1999: On the termination of El Niño. *Geophys. Res. Lett.,* **26,** 1593–1596.

——, and ——, 2001: El Niño and La Niña—Equatorial Pacific thermocline depth and sea surface temperature anomalies, 1986–98. *Geophys. Res. Lett.,* **28,** 1051–1054.

——, B. S. Giese, and E. S. Sarachik, 1990: Mechanisms of SST change in the equatorial waveguide during the 1982–83 ENSO. *J. Climate,* **3,** 173–188.

——, G. A. Vecchi, and R. H. Weisberg, 2000: Eastward surface jets in the central equatorial Pacific. November 1991–March 1992. *J. Mar. Res.,* **58,** 735–754.

Hendon, H. H., and M. L. Salby, 1994: The life cycle of the Madden–Julian oscillation. *J. Atmos. Sci.,* **51,** 2225–2237.

Jin, F. F., 1997: An equatorial ocean recharge paradigm for ENSO. Part I: Conceptual model. *J. Atmos. Sci.,* **54,** 811–829.

Kelly, K. A., S. Dickinson, M. J. McPhaden, and G. C. Johnson, 2001: Ocean currents evident in satellite wind data. *Geophys. Res. Lett.,* **28,** 2469–2472.

Klein, S. A., and D. L. Hartmann, 1993: The seasonal cycle of low stratiform clouds. *J. Climate,* **6,** 1587–1606.

Landsea, C. W., and J. A. Knaff, 2000: How much skill was there in forecasting the very strong 1997–98 El Niño? *Bull. Amer. Meteor. Soc.,* **81,** 2107–2119.

Large, W. G., and S. Pond, 1981: Open-ocean momentum-flux measurements in moderate to strong winds. *J. Phys. Oceanogr.,* **11,** 324–336.

——, and ——, 1982: Sensible and latent heat-flux measurements over the ocean. *J. Phys. Oceanogr.,* **12,** 464–482.

Larkin, N. K., and D. E. Harrison, 2002: ENSO warm (El Niño) and cold (La Niña) event life cycles: Ocean surface anomaly patterns, their symmetries, asymmetries, and implications. *J. Climate,* **15,** 1118–1140.

Lengaigne, M., J.-P. Boulanger, C. Menkes, P. Delecluse, and J. Slingo, 2004: Westerly wind events in the tropical Pacific and their influence on the coupled ocean-atmosphere system: A review. *Earth Climate: The Ocean-Atmosphere Interaction, Geophys. Monogr.,* Vol. 147, Amer. Geophys. Union, 49–69.

——, ——, ——, and H. Spencer, 2006: Influence of the seasonal cycle on the termination of El Niño events in a coupled general circulation model. *J. Climate,* **19,** 1850–1868.

Levitus, S., 1982: *Climatological Atlas of the World Ocean.* NOAA Prof. Paper 13, 173 pp. and 17 microfiche.

Madden, R. A., and P. R. Julian, 1994: Observations of the 40–50 day tropical oscillation—A review. *Mon. Wea. Rev.,* **122,** 814–837.

McPhaden, M. J., 1993: TOGA-TAO and the 1991–93 El Niño-Southern Oscillation Event. *Oceanography,* **6,** 36–44.

——, 1999: Genesis and evolution of the 1997–98 El Niño. *Science,* **283,** 950–954.

——, and X. Yu, 1999: Equatorial waves and the 1997–98 El Niño. *Geophys. Res. Lett.,* **26,** 2961–2964.

——, and Coauthors, 1998: The Tropical Ocean-Global Atmosphere (TOGA) observing system: A decade of progress. *J. Geophys. Res.,* **103,** 14 169–14 240.

Moore, D. W., and S. G. H. Philander, 1977: Modeling the tropical oceanic circulation. *The Sea,* E. D. Goldberg et al., Eds., Ocean Engineering Science, Vol. 6, Wiley Interscience, 319–361.

Neelin, J. D., D. S. Battisti, A. C. Hirst, F. F. Jin, Y. Wakata, T. Yamagata, and S. E. Zebiak, 1998: ENSO theory. *J. Geophys. Res.,* **103** (C7), 14 261–14 290.

Nicholls, N., and A. Kariko, 1993: East Australian rainfall events: Interannual variations, trends, and relationships with the Southern Oscillation. *J. Climate,* **6,** 1141–1152.

Pacanowski, R. C., and S. G. H. Philander, 1981: Parameterizations of vertical mixing in numerical models of tropical oceans. *J. Phys. Oceanogr.,* **11,** 1443–1451.

Philander, S. G. H., and A. D. Seigel, 1985: Simulation of the El Niño of 1982–1983. *Coupled Ocean Atmosphere Models,* J. Nihoul, Ed., Elsevier, 517–541.

Picaut, J., M. Ioualalen, C. Menkes, T. Delcroix, and M. McPhaden, 1996: Mechanisms of the zonal displacements of the Pacific warm pool: Implications for ENSO. *Science,* **274,** 1486–1489.

——, F. Masia, and Y. du Penhoat, 1997: An advective-reflective conceptual model for the oscillatory nature of ENSO. *Science,* **277,** 663–666.

——, E. Hackert, A. J. Busalacchi, R. Murtugudde, and G. S. E. Lagerloef, 2002: Mechanisms of the 1997–1998 El Niño–La Niña, as inferred from space-based observations. *J. Geophys. Res.,* **107,** 3037, doi:10.1029/2001JC000850.

Radenac, M.-H., and Coauthors, 2001: Modeled and observed impacts of the 1997–98 El Niño on nitrate and new production in the equatorial Pacific. *J. Geophys. Res.,* **106,** 26 879–26 898.

Rasmusson, E. M., and T. H. Carpenter, 1982: Variations in tropical sea surface temperature and surface wind fields associated with the Southern Oscillation/El Niño. *Mon. Wea. Rev.,* **110,** 354–384.

——, and J. M. Wallace, 1983: Meteorological aspects of the El Niño/Southern Oscillation. *Science,* **222,** 1195–1202.

Reynolds, R. W., and T. M. Smith, 1994: Improved global sea surface temperature analyses using optimum interpolation. *J. Climate,* **7,** 929–948.

——, N. A. Rayner, T. M. Smith, D. C. Stokes, and W. Wang, 2002: An improved in situ and satellite SST analysis for climate. *J. Climate,* **15,** 1609–1625.

Rosati, A., K. Miyakoda, and R. Gudgel, 1997: The impact of ocean initial conditions on ENSO forecasting with a coupled model. *Mon. Wea. Rev.,* **125,** 754–772.

Spencer, H., 2004: Role of the atmosphere in seasonal phase locking of El Niño. *Geophys. Res. Lett.,* **31,** L24104, doi:10.1029/2004GL021619.

Strutton, P. G., and F. P. Chavez, 2000: Primary productivity in the equatorial Pacific during 1997–98 El Niño. *J. Geophys. Res.,* **105** (C11), 26 089–26 101.

Suarez, M. J., and P. S. Schopf, 1988: A delayed action oscillator for ENSO. *J. Atmos. Sci.,* **45,** 3283–3287.

Takayabu, Y. N., T. Iguchi, M. Kachi, A. Shibata, and H. Kanzawa, 1999: Abrupt termination of the 1997–98 El Niño in response to a Madden-Julian Oscillation. *Nature,* **402,** 279–282.

Vecchi, G. A., 2006: The termination of the 1997–98 El Niño. Part II: Mechanisms of atmospheric change. *J. Climate,* **19,** 2647–2664.

——, and D. E. Harrison, 2000: Tropical Pacific sea surface temperature anomalies, El Niño, and equatorial westerly wind events. *J. Climate,* **13,** 1814–1830.

——, and ——, 2003: On the termination of the 2002–03 El Niño event. *Geophys. Res. Lett.,* **30,** 1964, doi:10.1029/2003GL017564.

——, A. Rosati, and D. E. Harrison, 2004: Setting the timing of El Niño termination. *Bull. Amer. Meteor. Soc.,* **85,** 1065–1066.

Vialard, J., C. Menkes, J.-P. Boulanger, P. Delecluse, E. Guilyardi, M. J. McPhaden, and G. Madec, 2001: A model study of oceanic mechanisms affecting equatorial Pacific sea surface temperature during the 1997–98 El Niño. *J. Phys. Oceanogr.,* **31,** 1649–1675.

Wang, B., R. Wu, and R. Lukas, 1999: Roles of the western North Pacific wind variation in thermocline adjustment and ENSO phase transition. *J. Meteor. Soc. Japan,* **77,** 1–16.

Wang, C., 2001: A unified oscillator model for the El Niño–Southern Oscillation. *J. Climate,* **14,** 98–115.

——, and R. H. Weisberg, 2000: The 1997–98 El Niño evolution relative to previous El Niño events. *J. Climate,* **13,** 488–501.

——, and J. Picaut, 2004: Understanding ENSO physics—A review. *Earth Climate: The Ocean-Atmosphere Interaction, Geophys. Monogr.,* Vol. 147, Amer. Geophys. Union, 21–48.

Wang, W., and M. J. McPhaden, 2001: Surface layer temperature balance in the equatorial Pacific during the 1997–98 El Niño and 1998–99 La Niña. *J. Climate,* **14,** 3393–3407.

Weare, B. C., A. R. Navato, and R. E. Newell, 1976: Empirical orthogonal analysis of Pacific sea surface temperatures. *J. Phys. Oceanogr.,* **6,** 671–678.

Weisberg, R., and C. Wang, 1997: A western Pacific oscillator paradigm for the El Niño-Southern Oscillation. *Geophys. Res. Lett.,* **24,** 779–782.

Wilson, C., and D. Adamec, 2001: Correlations between surface chlorophyll and sea surface height in the tropical Pacific during the 1997–99 El Niño-Southern Oscillation event. *J. Geophys. Res.,* **106** (C12), 31 175–31 188.

Woodruff, S. D., R. J. Slutz, R. L. Jenne, and P. M. Steurer, 1987: A Comprehensive Ocean-Atmosphere Data Set. *Bull. Amer. Meteor. Soc.,* **68,** 1239–1250.

Wyrtki, K., 1975: El Niño—The dynamic response of the equatorial Pacific Ocean to atmospheric forcing. *J. Phys. Oceanogr.,* **5,** 572–584.

Zebiak, S. E., and M. A. Cane, 1987: A model El Niño–Southern Oscillation. *Mon. Wea. Rev.,* **115,** 2262–2278.

Zelle, H., G. Appeldoorn, G. Burgers, and G. J. van Oldenborgh, 2004: The relationship between sea surface temperature and thermocline depth in the eastern equatorial Pacific. *J. Phys. Oceanogr.,* **34,** 643–655.

Zhang, X., and M. J. McPhaden, 2006: Wind stress variations and interannual sea surface temperature anomalies in the eastern equatorial Pacific. *J. Climate,* **19,** 226–241.